SAG: Stars and Galaxies **Vol. 7**, id. 6, 2024 December 28

Astrometric Search for Open Clusters and Associations around Binaries with Early Type Primaries

Yoichi ITOH[1,*]
[1]*Center for Astronomy, University of Hyogo, Nishi-Gaichi, Sayo, Hyogo 679-5313, Japan*
[*]*yitoh@nhao.jp*

(Received 2024 October 31; accepted 2024 December 10)

Abstract

In this study, we present result of astrometric search for open clusters and associations around an early-type primary star in a binary or multiple star system. Based on the position, parallax, and proper motion measured by $Gaia$ satellite, 98 open clusters and 110 associations were identified. Among them, 109 clusters and associations are newly discovered. The number of the membership ranged from 8 to 1526. The ages of the open clusters and associations were estimated to be between $10^{6.3}$ yr and $10^{8.9}$ yr. It is indicated that most of early-type stars are born in a stellar cluster with a number of low-mass stars. The low-mass stars in the open clusters and associations are candidates of post T Tauri stars.

Key words: open clusters and associations: general — parallaxes — proper motions

1. Introduction

Many observational characteristics of pre-main sequence stars are attributed to a proto-planetary disk. For example, infrared excess of protostars and classical T Tauri stars is thermal emission of dusts in a protoplanetary disk. Furthermore, hydrogen emission lines observed for classical T Tauri stars and weak-line T Tauri stars are generated by accretion shock of materials from a protoplanetary disk to the photosphere of the central star.

When dusts in a protoplanetary disk coagulate into planetesimals, dusts are evaporated by strong UV radiation of the central star, and/or dusts are blown out by the stellar wind, the observational characteristics of pre-main sequence stars also weaken. As a result, such an object is hard to be identified as a pre-main sequence star. Objects after the weak-line T Tauri stars but have not reached the main sequence yet correspond to such objects. They are called post T Tauri stars. Because post T Tauri stars are few times older than weak-line T Tauri stars, one imagines that the number of post T Tauri stars is several times larger than that of weak-line T Tauri stars (see e.g., Jensen 2001).

However, the number of the post T Tauri stars so far discovered is very small. Several attempts have been conducted to address this deficiency problem of post T Tauri stars. Gahm, Ahlin, and Lindroos (1983) identified 254 visual binaries and multiple systems of which primary star is an O- or B-type star (early-type primary binary systems, hereafter called as the EP binaries). Among them, Lindroos (1986) focused on the EP binaries whose secondary star is an F-, G-, or K-type star. Because lifetime of an early-type main-sequence star is very short, the secondary of the EP binaries should be young as few tens million years old. Lindroos (1986) considered these secondaries as candidates of post T Tauri stars.

As pointed out by Lada, Strom, and Myers (1993), most of the stars in the Galaxy are born in clusters. Approximately 80 % of O-type stars are associated with stellar cluster and/or OB associations. We expect a young open cluster also around the EP binaries. The member of an open cluster should have common distance, proper motion, age, and chemical composition.

Several studies have been conducted for discovering stellar cluster around O-type stars. Approximately 20 % of O-type stars are known to be field stars. de Wit et al. (2004) conducted near-infrared K-band imaging observations around 43 O-type field stars in the Galaxy. They investigated stellar density enhancements in 5 $\times$ 5 arcmin^2 regions centered on the O-type stars. They identified stellar clusters around 5 O-type stars, and concluded that majority of the O-type field stars are isolated. de Wit, Testi, and Palla (2005) proposed that the isolated O-type stars are dynamically ejected from young stellar clusters. They confirmed this possibility as the high fraction of the O-type field stars have large space velocity and/or large distance from the Galactic plane.

We have carried out astrometric search for open clusters and associations centered on the primary star of the binary systems listed in Gahm, Ahlin, and Lindroos (1983). By using precise astrometric data taken with the Gaia satellite, significant number of open clusters and associations are newly identified.

2. Data Analysis

We searched for stellar clusters and associations (hereafter we call groups) around 254 EP binaries listed in Gahm, Ahlin, and Lindroos (1983). The primary star of the binary is an early-type star, and located at the center of the searched region. We used the Gaia DR3 archive (Gaia Collaboration et al. 2016,

2023) for coordinates, parallax, proper motion, apparent magnitude, $B_\mathrm{P} - R_\mathrm{P}$ color, and amount of the extinction at G-band of an object.

We constructed the selection criteria for group members, by assuming IC 2391 as the template of the groups. Nisak et al. (2022) investigated the membership of IC 2391 cluster and used the Gaia DR2 catalog. They set the criteria on uncertainties in the parallax and proper motion. For the object with G-band magnitude brighter than 8.0, uncertainty of parallax measurement should be less than 0.5 mas. For the other objects, the uncertainty should be less than 0.35 mas. Uncertainties of proper motion measurements should be less than 0.8 mas yr^{-1} for R.A. and Dec. directions. Subsequently, they found 350 cluster member candidates of IC 2391. The astrometric properties of the IC 2391 members are as follows; the standard deviations of the R.A. and Dec. of the members are 1.630 degree and 1.763 degree, which correspond to 4.29 pc and 4.64 pc, respectively. The standard deviation of the parallax of the members is 0.228 mas (Nisak et al. 2022), which corresponds to 4.99 pc. The standard deviation of the proper motions of the members are 1.59 mas yr^{-1} and 1.61 mas yr^{-1} for the R.A. and Dec. directions, respectively. Those correspond to 1.2×10^{-6} pc yr^{-1}.

Based on these astrometric properties, we searched the objects within 15 pc from the primary star of the EP binaries. We considered an object to be a group member candidates, if the proper motion differences of the object and the primary are less than 3.6×10^{-6} pc yr^{-1} for the R.A. and Dec. directions.

Several recent studies have employed data-mining techniques and machine-learning algorithms for detecting open clusters. DBSCAN is a density-based clustering algorithm (e.g., Castro-Ginard et al. 2018). Distance between two stars is calculated on 5 dimensional space (positions, parallax, proper motions), and then over-density region in the 5D space are searched. The minimum spanning tree method is another method to find clumps and filaments (e.g., Gutermuth et al. 2009). The tree is constructed by joining nearest two points, such that the total length of all the lines is minimized. Combination of DBSCAN and the minimum spanning tree method, called HDBSCAN, is recently used for clustering search (e.g., Hunt & Reffert 2021). These methods are efficient for unbiased search for clusters. On the other hand, in this study, we focused on stellar clusters around primary star of the EP binaries. Because the primary star is the most massive object in the cluster, we considered that its position, proper motion and distance from the Earth are close to mean of those of the cluster members. Therefore, our study is heavily biased; thus we employed simple approach for searching for a stellar cluster and association centered on the primary star of the EP binaries.

3. Results

We searched for group members around 254 early-type primary stars in the EP binaries. Among them, the parallax and proper motion of 243 primaries are listed in the Gaia DR3 catalog.

There is no rigid definition on the minimum number of cluster member. Different studies have set different minimum number. We set the minimum number of the group member to be 8, as that in Castro-Ginard et al. (2018). Groups are found around 208 primaries (Table 1). We claim that the majority of the primary stars listed in Gahm, Ahlin, and Lindroos (1983) are indeed associated with stellar groups. We identified 18906 objects around 208 primaries as the candidates of the group members. Number of the group member candidates is 90.9 in average, and 27.5 in median.

HD 74146 is the primary star of an EP binary in IC 2391 cluster. We identified 377 objects as cluster member candidates around HD 74146. Among them, 59 objects are not listed in Nisak et al. (2022). Fifteen objects among the 59 objects are located out of the searched region of Nisak et al. (2022). We consider that a part of the discrepancy in the membership identification is caused by the difference between Gaia DR2 and DR3 catalogs. Nisak et al. (2022) listed 350 objects as the cluster members. Among them, 31 objects were not identified as the candidates in our study. Eleven objects among 31 objects are located beyond 15 pc from HD 74146. We considered that the completeness of the membership identification is approximately 90 %.

Figure 1 shows the color-magnitude diagram of IC 2391 cluster. B_P - R_P color of each star is corrected for interstellar extinction. We used the relationship between interstellar extinction and interstellar reddening given by Bromley et al. (2018). The absolute magnitude of an object was calculated with an apparent G-band magnitude and the parallax with correction of interstellar reddening. The figure shows coeval formation of the cluster members.

Lindroos (1986) selected 78 binary or multiple star systems as certain physical systems. Among them, secondary star of 45 systems have the spectral types later than F0. They considered that these stars are probable candidates of post T Tauri stars. We noticed that 26 objects out of 45 objects have the astrometric measurements with Gaia. Among them 13 objects have common parallax and proper motions to those of the primaries (HD 560B, HD 1438B, HD 8803B, HD 23793B, HD 53191B, HD 60102B, HD 63465B, HD 74146B, HD 77484B, HD 86388B, HD 108767B, HD 113703B, HD 143939B).

4. Discussion

4.1. RUWE of the primary stars

RUWE (renormalized unit weight error) is an indicator of the PSF shape of an object in the Gaia catalog. The Gaia catalog indicates that the source is non-single or problematic for the astrometric solution if RUWE is larger than ~ 1.4. We examined whether detection rates of the group member candidates depend on RUWE of the primary star. For the primary stars with RUWE less than 1.4, 64 secondary stars are identified as the group member candidates, whereas 106 secondaries are not identified as the candidates. The average number of the group member candidates is 94, and 28 groups have more than 100 candidates for such primaries. On the other hand, for the primary stars with RUWE larger than 1.4, 22 secondary stars are identified as the group member candidates, whereas 51 secondaries are not identified as the candidates. The average number of the group member candidates is 83, and 11 groups have more than 100 candidates for such primaries. We did not obtain sig-

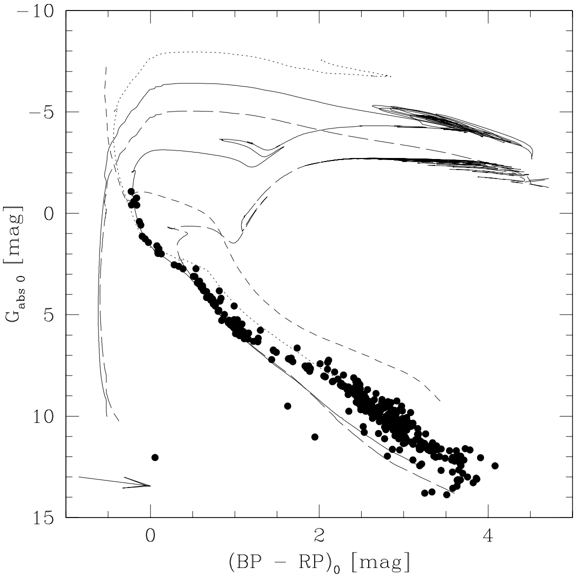

Fig. 1. Color-magnitude diagram of the cluster member candidates of the IC 2391 cluster. The horizontal axis shows $B_{\rm P}$ - $R_{\rm P}$ color corrected for interstellar extinction. The vertical axis shows the absolute magnitude at the G-band. The arrow at bottom left indicates interstellar extinction with $A_{\rm V}$ = 1 mag. Short-dashed, dotted, solid, and long-dashed lines represent isochrones of 1 Myr, 10 Myr, 100 Myr, and 1 Gyr, respectively.

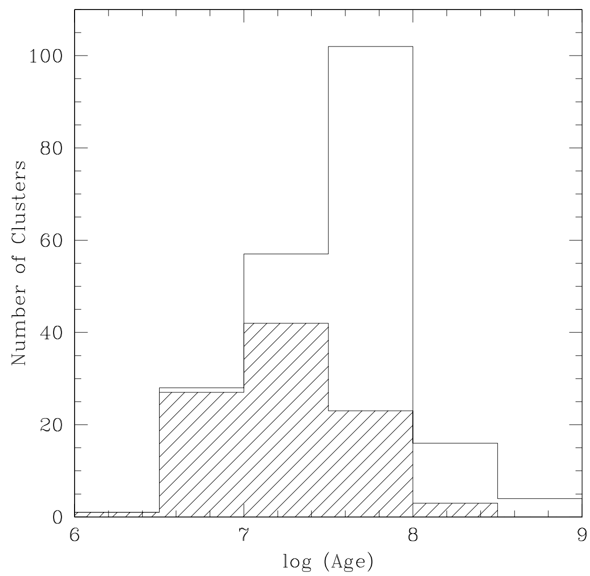

Fig. 2. Age distribution of the open clusters (hatched histogram) and associations (unhatched histogram). The age of the cluster and association is estimated with isochrones on the color-magnitude diagram.

nificant difference for detection rates and group properties for different RUWE samples of the primaries.

4.2. *Open cluster or Association*

Here, we examine whether the stellar groups around the OB stars are gravitationally bound. If bound, the group is called an open cluster. Otherwise, it is classified into an association (Portegies Zwart et al. 2010). Gravitational energy of a stellar group, U, is written as

$$U = -\frac{GM^2}{R}, \tag{1}$$

where M is the total mass of the group. We assumed the sum of the mass of the group member candidates as the total mass. We used MIST evolutionary tracks (Dotter 2016; Choi et al. 2016; Paxton et al. 2011; Paxton et al. 2013; Paxton et al., 2015) with the age between 0.1 Myr and 1 Gyr with the steps of 0.1 dex for the mass estimation of each member candidate. R is the radius of the group. We considered the mean distance between the group member candidate and the primary as the radius of the group. T is the sum of the kinematic energy of the star,

$$T = \sum \frac{1}{2} m v^2, \tag{2}$$

where m is the mass of a group member candidate and v is the velocity of the candidate. The velocity of each candidate is expressed as

$$v = \sqrt{2} \times \sqrt{(v_{\rm RA} - v_{\rm RA,P})^2 + (v_{\rm Dec} - v_{\rm Dec,P})^2}, \tag{3}$$

where $v_{\rm RA}$ and $v_{\rm Dec}$ are the velocities of the candidate in R.A. and Dec. directions, respectively, and $v_{\rm RA,P}$ and $v_{\rm Dec,P}$ are the velocities of the primary star of the EP binary in R.A. and Dec. directions, respectively. Velocities are calculated from proper motion and parallax of the object. If $2T + U < 0$, the group is bound; hence it is an open cluster. Otherwise, the group is unbound; hence it is an association. Consequently, we identified 98 open clusters and 110 associations.

4.3. *Age of clusters and associations*

The ages of the clusters and associations are estimated by comparing colors and magnitudes of the group member candidates and isochrones on color-magnitude diagrams. We determined the age of the group if the least square was the minimum between the object points and the isochrones. Figure 2 shows age distribution of all groups. Most of the groups have the ages of the order of 10 Myr. We think that this age distribution is considerably biased. The most massive star already leaves the main sequence, if the cluster is old. The most massive star is not identified as an early-type star in this case. A 2 $M_\odot$ star (latest B-type star) leaves main-sequence at 100 Myr.

It is indicated that the clusters are younger than the associations. Therefore, a less-massive cluster is short-lived and a part of the associations are indeed disrupting open clusters.

Age of open clusters has extensively been investigated. Anders et al. (2021) constructed the cluster age function of 834 open clusters in a 2 kpc cylinder around the Sun by employing Gaia DR2 catalog. They found that the cluster age function has a peak at log $t \sim 8.2$. This age function is well fitted with the age function derived from tidal destruction model of Lamers et al. (2005). This model considered that an open cluster is disrupted by mass loss of evolved stars and tidal stripping of the Galaxy. The disruption timescale is derived as 1.3 $\pm$ 0.5 Gyr for a 10^4 $M_\odot$ cluster in solar neighborhood.

Figure 3 shows the number of the group member candidates

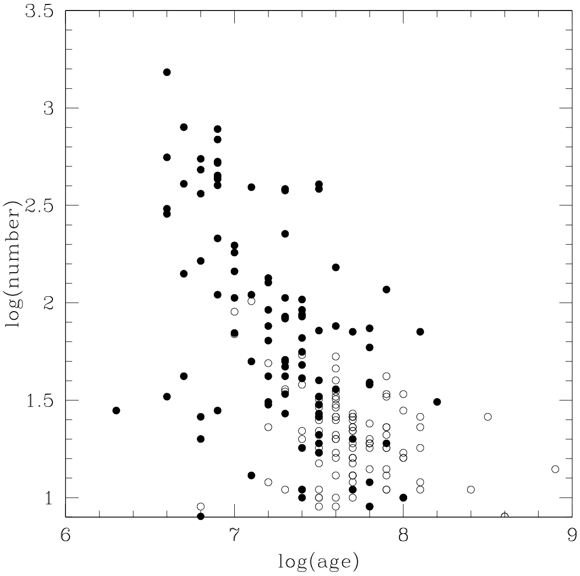

Fig. 3. Number of the cluster member candidates as a function of the group age. Filled circles represent the open clusters and open circles represent the associations.

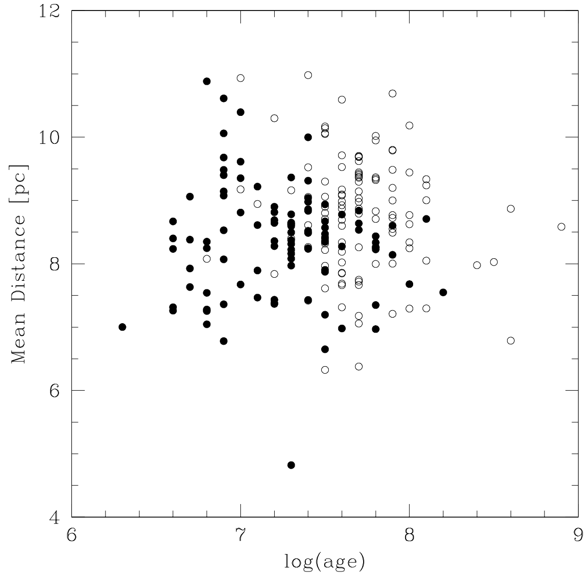

Fig. 4. Mean distance of the cluster member candidates and the primary star as a function of the group age. Filled circles and open circles represent the open clusters and the associations, respectively.

as a function of the group age. One notices that the clusters are richer and younger than the associations. The number of the candidates decreases with increasing age. This appears to be disruption process of the open clusters and associations. Figure 4 shows the mean distance of the cluster member candidates from the primary as a function of the age of the cluster. There is no strong trend on the mean distance and no significant difference between the clusters and the associations. We considered that the cluster expands with age, so that a fraction of the cluster member candidates are located beyond 15 pc from the primary, and then the cluster are gravitationally unbound, recognized as an association.

4.4. *Spatial distribution of the member candidates*

Spatial distribution of the cluster member candidates was investigated. We selected 20 rich open clusters whose member candidates are exceeding 300, then divided the candidates into two groups. Objects with the B_P - R_P color less than 1.0 magnitude are classified into the early type group. Objects with the B_P - R_P color equal to or larger than 1.0 magnitude are classified into the late type group. Subsequently, we constructed cumulative number distribution by distance of the group member candidates and the primary for each cluster. The P-value of the Kolmogorov-Smirnov test was larger than 0.87 for all clusters, indicating that there was no significant difference between two groups. We did not find any evidence for mass segregation of the clusters. Note that most of the rich clusters are young. We consider that the mass segregation does not occur, at least, in such young clusters.

Figure 5 shows proper motion differences between the cluster member candidates of IC 2391 cluster and HD 74146. The proper motion differences are larger for the cluster member candidates located far from HD 74146. Among the rich clusters, 5 clusters, HD 74146, HD 106983, HD 112092, HD 113703, and HD 150742, show large proper motion differences for the peripheral members. This trend may indicate disruption process of the cluster.

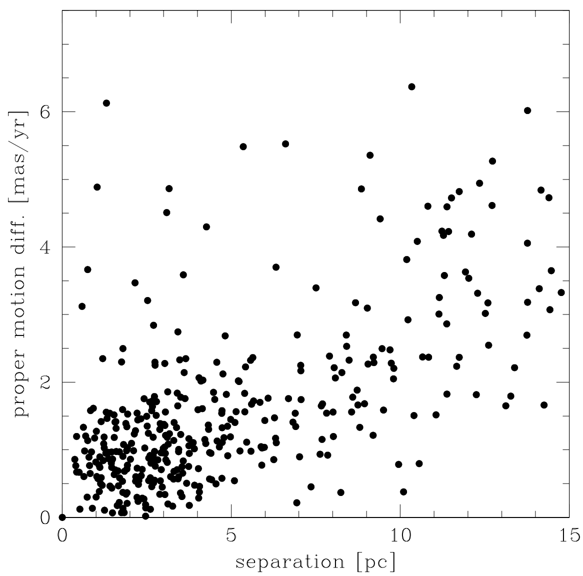

Fig. 5. Difference of proper motions between the cluster member candidates and the primary of the EP binary, HD 74146, in the IC 2391 cluster.

The Jacobi radius is the distance between the cluster center and L_1 or L_2 Lagrange point, which is defined as

$$r_{\rm J} = \left(\frac{GM}{2\omega^2}\right)^{\frac{1}{3}}, \tag{4}$$

where $\omega = V_{\rm G}/R_{\rm G}$. $V_{\rm G}$ and $R_{\rm G}$ are the galactocentric distance and circular orbital speed of the cluster around the Galaxy center. For the IC 2391 cluster, we derived $r_{\rm J}$ = 8.7 pc. It means that objects located at more than 8.7 pc away from the cluster center are escaping from the cluster to field. Objects with large separation tend to be accelerated and to have large proper motion difference, indicating disruption process of the cluster by Galactic tidal force.

A large fraction of the cluster member candidates have large $B_{\rm P}$ - $R_{\rm P}$ color, indicating late spectral type, and age of several tens Myr. These are potential objects of post T Tauri stars. Gravitational instability model of planet formation process predicts that a Jovian planet forms within 1 Myr after the formation of a star. Various shapes of circumstellar disks with grooves, such as the disk around HL Tau, may indicate Jovian planet formation by gravitational instability. On the other hand, core accretion model predicts that rocky planets form in $\sim$ 100 Myr after star formation. Inutsuka, Machida, and Matsumoto (2010) proposed a hybrid model of planet formation. They predict formation of Jovian planets less than 1 Myr by gravitational instability, because the central star is not massive enough to prevent from fragmentation of a circumstellar disk. As the central star grows, terrestrial planets form in the circumstellar disk by aggregation of dusts and planetesimals. It is generally believed that a terrestrial planet forms $\sim$ 100 Myr after the formation of the star. Newly-born terrestrial planets may orbit the member candidates of the open clusters and associations discovered in this study.

5. Conclusions

We searched for objects with similar positions, parallax, and proper motions around the early-type primary star of a binary systems. We identified 18906 objects around 208 primaries as the member candidates of open clusters and associations. The age of the clusters and associations were estimated to be between $10^{6.3}$ yr and $10^{8.9}$ yr. Therefore, they are considered as possible candidates of post T Tauri stars. Consequently, we propose evolution sequence of a stellar group that a tightly aggregated rich open cluster changes to a loosely concentrated associations. Because a significant portion of the association members have gone away, we suggest that a certain fraction of post T Tauri stars are field stars.

This work has made use of data from the European Space Agency (ESA) mission *Gaia* (https://www.cosmos.esa.int/gaia), processed by the *Gaia* Data Processing and Analysis Consortium (DPAC, https://www.cosmos.esa.int/web/gaia/dpac/consortium). Funding for the DPAC has been provided by national institutions, in particular the institutions participating in the *Gaia* Multilateral Agreement. This work was supported by JSPS KAKENHI Grant Number 22K03677.

Appendix.

List of the group member candidates is presented in table 2. Full version of table 2 is published online.

References

Aarnio, A. N., Weinberger, A. J., Stassun, K. G., Mamajek, E. E., & James, D. J. 2008, AJ, 136, 2483
Alessi, B. S., Moitinho, A., & Dias, W. S. 2003, A&A, 410, 565
Anders, F., Cantat-Gaudin, T., Quadrino-Lodoso, I., Gieles, M., Jordi, C., Castro-Ginard, A., & Balaguer-Núñez, L. 2021, A&A, 645, L2
Bastian, U. 2019, A&A, 630, L8
Bica, E., Santiago, B. X., Dutra, C. M., Dottori, H., de Oliveira, M. R., & Pavani, D. 2001, A&A, 366, 827
Bromley, B. C., Kenyon, S. J., Brown, W. R., & Geller, M. J. 2018, ApJ, 868, 25
Buscombe, W., & Morris, P. M. 1960, MNRAS, 121, 263
Buscombe, W. 1962, MNRAS, 124, 189
Carrier, F., Burki, G., & Richard, C. 1998, A&A, 341, 469
Castro-Ginard, A., Jordi, C., Luri, X., Julbe, F., Morvan, M., Balaguer-Núñez, L., & Cantat-Gaudin, T. 2018, A&A, 618, A59
Cantat-Gaudin, T., et al. 2018, A&A, 618, A93
Choi, J., Dotter, A., Conroy, C., Cantiello, M., Paxton, B., & Johnson, B. D. 2016, ApJ, 823, 102
Clariá, J. J., Lapasset, E., Piatti, A. E., & Ahumada, A. V. 2003, A&A, 409, 541
de Geus, E. J., de Zeeuw, P. T., & Lub, J., 1989, A&A, 216, 44
de Geus, E. J., Lub, J., & van de Grift, E. 1990, A&AS, 85, 915
Denoyelle, J. 1977, A&AS, 27, 343
de Wit, W. J., Testi, L., Palla, F., Vanzi, L., & Zinnecker, H. 2004, A&A, 425, 937
de Wit, W. J., Testi, L., Palla, F., & Zinnecker, H. 2005, A&A, 437, 247
Dolgachev, V. P., Kalinina, E. P., & Kholopov, P. N. 1989, AZh, 66, 172
Dotter, A. 2016, ApJS, 222, 8
Eggen, O. J. 1974, PASP, 86, 241
Eggen, O. J. 1975, PASP, 87, 37
Eggen, O. J., 1992, AJ, 103, 1302
Feinstein, A. 1964, Obs., 84, 111
Feinstein, A. 1967, ApJ, 149, 107
Gahm, G. F., Ahlin, P., & Lindroos, K. P. 1983, A&AS, 51, 143
Gaia Collaboration (Prusti, T, et al.) 2016, A&A, 595, A1
Gaia Collaboration (Vallenari, A., et al.) 2023, A&A, 674, A1
Gagné, J., David, T. J., Mamajek, E. E., Mann, A. W., Faherty, J. K., & Bédard, A. 2020, ApJ, 903, 96
Gutierrez-Moreno, A., & Moreno, H. 1968, ApJS, 15, 459
Gutermuth, R. A., Megeath, S. T., Myers, P. C., Allen, L. E., Pipher, J. L., & Fazio, G. G. 2009, ApJS, 184, 18
Heske, A., & Wendker, H. J. 1985, A&A, 151, 309
Hunt, E. L., & Reffert, S. 2021, A&A, 646, A104
Inutsuka, S., Machida, M., & Matsumoto, T. 2010, ApJ, 718, L58
Jensen, E. L. N. 2001, in ASP conf. Ser., 244, ed. R. Jayawardhana & T. Greene (San Francisco: ASP), 3
Lada, E. A., Strom, K. M., & Myers, P. C. 1993, in Protostars and Planets III, ed. E. H. Levy & J. I. Lunine (Arizona: University of Arizona Press), 245
Lamers, H. J. G. L. M., Gieles, M., Bastian, N., Baumgardt, H., Kharchenko, N. V., & Portegies Zwart, S. 2005, A&A, 441, 117
Lindroos, K. P. 1986, A&A, 156, 223
Liu, J., Fang, M., & Liu, C. 2020, AJ, 159, 105
Loden, L. O. 1979, A&AS, 36, 83
Loden, L. O. 1980, A&AS, 41, 173
Madsen, S., Dravins, D., & Lindegren, L. 2002, A&A, 381, 446
Mel'nik, A. M., & Dambis, A. K. 2017, MNRAS, 472, 3887
Melnik, A. M., & Dambis, A. K. 2020, MNRAS, 493, 2339
Moffat, A. F. J., & Vogt, N. 1975, A&AS, 20, 125

Morris, P. M. 1961, MNRAS, 122, 325
Nisak, A. H., White, R. J., Yep, A., Henry, T. J., Paredes, L., James, H.-S., & Jao, W.-C. 2022, AJ, 163, 278
Ogura, K., & Ishida, K. 1975, PASJ, 27, 119
Paxton, B., Bildsten, L., Dotter, A., Herwig, F., Lesaffre, P., & Timmes, F. 2011, ApJS, 192, 3
Paxton, B., et al. 2013, ApJS, 208, 4
Paxton, B., et al. 2015, ApJS, 220, 15
Platais, I., Kozhurina-Platais, V., & van Leeuwen, F. 1998, AJ, 116, 2423
Portegies Zwart, S. F., McMillan, S. L. W., & Gieles, M. 2010, ARA&A, 48, 431
Thackeray, A. D., & Wesselink, A. J. 1965, MNRAS, 131, 121
van Genderen, A. M., Bijleveld, W., & van Groningen, E. 1984, A&AS, 58, 537
Walker, M. F. 1956, ApJS, 2, 365
Wolff, S. C., Strom, S. E., Dror, D., & Venn, K. 2007, AJ, 133, 1092
Zuckerman, B., Vican, L., Song, I., & Schneider, A. 2013, ApJ, 778, 5

Table 1. Candidates of open clusters around early-type binaries.

id.	Primary	Plx [mas]	PMra [mas yr^{-1}]	PMdec [mas yr^{-1}]	RUWE	member	binarity	log(age)	cl	reference
1	HD560	11.0592	31.4929	2.6513	0.73	12	y	7.7		Octans Near assoc. (Zuckerman et al. 2013)
2	HD1438	5.3927	23.3283	-2.7550	0.88	19	y	7.8		
3	HD3369	5.6563	14.6685	-3.3849	1.02	41	y	7.4	oc	
4	HD9899	4.3795	14.0856	-9.6563	1.00	30		7.6		
5	HD10161	4.0524	3.2529	6.6643	0.97	10	y	8.0		
6	HD10293	2.2799	13.1617	-7.1668	1.11	11	y	7.4		
7	HD16046	6.7146	-13.8432	-3.7901	1.80	14		7.9		
8	HD23793	7.3071	23.8477	-23.0900	1.12	87	y	7.4	oc	u Tau assoc. (Liu et al. 2020)
9	HD23990	6.7515	25.5435	-24.3792	0.93	106		7.3	oc	μ Tau assoc. (Gagné et al. 1983)
10	HD24388	4.1736	2.9425	-11.9696	2.84	16		7.7		
11	HD25330	6.4553	7.1991	0.6393	1.51	21	y	7.6		
12	HD27638	11.2029	20.8016	-17.0389	1.12	26		7.6		
13	HD28107	3.5126	1.3052	14.8570	1.57	18	y	7.8		
14	HD29227	3.1429	1.5206	-6.0844	1.23	11	y	7.3		
15	HD32202	3.5067	-7.6983	-12.0406	1.00	18	y	7.5		
16	HD32964	10.7278	9.3095	-0.5185	1.07	21		7.9		Ori OB1 (de Geus et al. 1990)
17	HD33224	4.9052	4.9131	-21.3372	1.08	14		7.8		
18	HD33802	14.1740	23.9310	-38.9331	2.40	20		7.4		
19	HD33949	6.9828	-12.4142	-1.3517	1.45	23		7.9		
20	HD34503	6.0147	-17.7267	-9.6123	4.14	26	y	8.1		
21	HD34527	3.8172	2.2405	0.7279	1.15	30	y	7.5		
22	HD34798	4.2465	0.7225	10.3636	1.05	23	y	7.2		
23	HD35007	3.3128	-0.7340	1.7512	7.00	102		7.1		Ori Ia (Wolff et al. 2007)
24	HD35149	1.8431	-1.8018	-3.4760	2.70	11		7.7	oc	Ori Ia (Wolff et al. 2007)
25	HD35173	2.9705	0.0745	-5.1494	1.63	76	y	7.2	oc	
26	HD35715	2.9943	1.0310	-1.0187	1.09	797		6.7	oc	Ori Ia (Wolff et al. 2007)
27	HD36013	2.7765	-0.6418	1.0750	1.15	548		6.8	oc	Ori Ia (Wolff et al. 2007)
28	HD36151	3.2899	0.5555	-1.7095	1.32	106		7.0	oc	Ori Ic (Wolff et al. 2007)
29	HD36408	2.8515	-4.0778	-10.5359	1.18	21	y	7.5	oc	
30	HD36779	2.7006	2.8040	-2.5399	1.16	558		6.6	oc	Ori Ib (Wolff et al. 2007)
31	HD36861	2.5936	2.8960	-3.1830	4.82	286	y	6.6	oc	λ Ori
32	HD36898	2.8710	-2.8134	-2.4529	2.73	85		7.3	oc	ASCC 19 (Cantat-Gaudin et al. 2018)

Table 1. (Continued.)

33	HD36960	2.6166	1.1105	1.6808	0.99	1526		6.6	oc	Orion Sword Cluster (Dolgachev et al. 1989)
34	HD38426	2.2645	0.1861	-1.0847	1.11	9		7.6		
35	HD38622	3.4599	4.9596	-11.4889	0.93	48	y	7.4	oc	local assoc.(Eggen 1975)
36	HD38672	2.9934	-4.3587	-8.9225	0.94	40		7.5	oc	
37	HD40494	3.0918	-2.6517	10.2178	1.11	12		7.8	oc	
38	HD43286	3.1601	-4.4303	-3.8110	0.94	127		7.2	oc	HIP29713 cluster (Platais et al. 1998)
39	HD43983	2.7061	1.9275	-4.9152	1.28	26	y	7.5		
40	HD44458	1.8635	-2.2725	1.1927	0.82	17		7.5	oc	
41	HD44944	5.3697	-2.8473	-1.5546	2.71	26		7.7		
42	HD44996	2.5024	-3.8176	2.7741	0.86	83	y	7.3	oc	
43	HD46035	4.0487	-2.5337	0.4440	5.33	30		7.5	oc	CMa OB1 (de Geus et al. 1990)
44	HD46064	2.1584	-3.2894	1.1535	1.03	22		7.7		CMa OB1 (de Geus et al. 1990)
45	HD46547	1.3656	-3.4638	4.6922	1.03	10		7.4	oc	
46	HD47116	2.9558	-0.1677	4.9850	1.07	18		7.7		CMa OB1 (de Geus et al. 1990)
47	HD47247	3.2979	-7.9475	7.8803	0.97	66	y	7.4	oc	CMa OB1 (de Geus et al. 1990)
48	HD47732	1.3885	-1.9428	-3.7751	1.09	304		6.6	oc	NGC2264 (Walker 1956)
49	HD47851	1.4128	-2.7925	4.4405	1.04	12		7.2		
50	HD47887	1.2104	-2.7517	-3.9136	0.96	33		6.6	oc	NGC2264 (Walker 1956)
51	HD48383	3.5624	-4.8955	11.0181	1.14	32	y	7.6		
52	HD48425	2.3768	-4.6318	6.2080	1.00	92		7.2	oc	Sco-Cen (Buscombe 1962)
53	HD48857	2.1131	-6.7853	10.1406	1.01	42	y	7.3	oc	
54	HD48917	1.6454	-3.2862	4.2006	1.09	19		7.5	oc	Collinder 121 (Feinstein 1967)
55	HD52140	4.0874	-11.2418	7.2875	0.99	85		7.4	oc	Collinder 121 (Feinstein 1967)
56	HD52437	0.7882	-2.6651	2.8485	8.41	11		7.9		CMa OB1 (de Geus et al. 1990)
57	HD53191	4.4210	1.7749	18.3337	1.01	17	y	8.0		
58	HD53755	0.9091	-4.3423	1.6201	1.02	42	y	6.7	oc	Alessi 21 (Cantat-Gaudin et al. 2018)
59	HD55856	1.3890	-3.9609	3.3707	1.06	51		7.3	oc	CMa OB1 (de Geus et al. 1990)
60	HD56456	9.0489	-4.2718	-0.1516	0.77	40		7.6		Alessi 3 (Alessi et al. 2003)
61	HD56504	1.4662	-3.7507	4.4162	2.63	42		7.2	oc	
62	HD58420	4.4519	-10.7414	18.8006	1.05	23		8.1		

Table 1. (Continued.)

63	HD60102	5.1936	-10.7465	12.3498	1.00	19	y	7.7		
64	HD60624	2.0348	-6.9713	0.7783	0.87	384		7.5	oc	NGC2422 (Cantat-Gaudin et al. 2018)
65	HD60855	2.0401	-7.1076	0.5415	1.10	406	y	7.5	oc	NGC2422 (Cantat-Gaudin et al. 2018)
66	HD60863	13.6185	-60.2559	-7.7415	1.65	11		8.1		
67	HD61555	9.0301	-18.5565	11.0805	2.32	24		7.8		
68	HD63065	3.3336	1.9171	-4.5255	0.99	152	y	7.6	oc	Herschel 1 (Bica et al. 2001)
69	HD63425	0.9832	-1.6790	5.2319	0.99	10		8.0		
70	HD63465	2.7053	-9.4330	4.8647	0.99	392	Y	7.1	oc	NGC2451 (Carrier et al. 1999)
71	HD63922	3.5065	-6.9691	6.6364	6.01	23		7.9		
72	HD65162	1.1831	-5.2888	5.1679	1.05	26	y	7.5	oc	
73	HD66005	2.5463	-5.4350	8.1857	0.98	363	y	6.8	oc	
74	HD66230	1.7505	-7.1821	1.4007	3.94	11		7.7		
75	HD66539	0.8744	-4.9056	2.4670	0.99	10	y	8.0	oc	
76	HD66546	2.1702	-5.7762	6.2200	2.91	47	y	7.3	oc	Sco-Cen (Morris 1961)
77	HD66624	6.7621	-5.8699	15.0247	1.34	18		7.9		local assoc. (Eggen 1974)
78	HD67059	1.0395	-2.3700	4.2190	0.92	13		7.7		
79	HD67880	3.1861	-8.3424	-4.9380	0.90	26		7.7		
80	HD69144	2.7446	-8.1434	10.3565	1.02	408		6.7	oc	Vela OB2 (Mel'nik & Dambis 2017)
81	HD70309	2.9211	-14.1356	11.1898	1.03	54		7.4		
82	HD70556	2.3493	-7.2993	7.1496	1.17	110	y	7.1	oc	
83	HD71510	4.3147	-14.4705	17.4617	0.86	50		7.3	oc	
84	HD72798	1.4732	-9.2406	9.3108	0.81	27		7.3	oc	
85	HD74067	13.1970	-57.2076	6.6014	3.42	18	y	7.9		Vela (Denoyelle 1977)
86	HD74115	3.1062	-13.0543	11.1637	1.02	17		7.5		Trumpler 10 (Cantat-Gaudin et al. 2018)
87	HD74146	6.5580	-24.7958	23.3729	1.07	377	y	7.3	oc	IC 2391 (Nisak et al. 2022)
88	HD74531	1.4345	-4.2424	2.4137	1.11	141	y	6.7	oc	IC 2395 (Clariá et al. 2003)
89	HD76566	2.6833	-13.0909	7.6006	0.98	84		7.3	oc	Platais 9 (Cantat-Gaudin et al. 2018)
90	HD77002	5.1705	-8.6512	9.2236	0.90	20	y	7.7		Sco-Cen (Buscombe & Morris 1960)
91	HD77484	4.0669	-15.9890	-3.4409	0.97	11	y	7.5		
92	HD82906	3.0733	-19.1766	-9.0391	1.02	9		7.8		
93	HD83953	5.9358	-28.9825	3.1454	1.05	28		8.0		local assoc. (Eggen 1975)
94	HD86440	1.9030	-13.3781	4.1097	2.45	32		7.5		Sco OB2-5 (de Geus et al. 1990)

Table 1. (Continued.)

95	HD90972	7.0076	-29.5984	1.7039	2.33	23		7.7		
96	HD91355	3.9659	-14.3904	-1.2000	1.08	27	y	7.7		
97	HD91590	5.7481	-19.6953	7.8553	16.29	13		7.7		
98	HD91645	4.0374	-18.2411	3.4498	1.14	15		7.5		
99	HD92029	2.8313	-13.7781	4.7828	1.01	29		7.5		
100	HD93010	2.4570	-15.4085	2.9948	0.83	384	y	7.3	oc	Alessi 5 (Alessi et al. 2003)
101	HD93632	0.4049	-6.4421	1.9229	0.83	26	y	6.8	oc	Bochum 11 (Moffat & Vogt 1975)
102	HD94565	3.5994	-31.1929	7.8720	1.77	16	y	8.0		
103	HD95198	2.6791	-22.5129	-0.4316	0.95	10		7.6		
104	HD96261	0.5222	-6.0838	2.2165	3.68	42		7.9		Feinstein 1 (Feinstein 1964)
105	HD96264	0.3292	-6.4926	1.5838	0.89	11		7.4	oc	Loden 306 (Loden 1980)
106	HD97583	10.2398	-47.5188	5.5451	0.93	25		7.5		Sco-Cen ((Morris 1961))
107	HD99803	5.8843	-38.4008	8.8323	1.90	26		7.6		
108	HD100359	2.4492	-6.4095	1.5162	5.08	9		7.8		
109	HD100841	8.2770	-33.8629	-7.2356	2.61	110		6.9	oc	lower Centaurus Crux assoc. (Madsen et al. 2002)
110	HD101436	0.6195	-5.2118	0.9749	2.12	18		7.4	oc	IC2944 (Thackeray & Wesselink 1965)
111	HD102340	0.9783	-9.3064	0.9579	1.18	19	y	7.9	oc	Sco OB2-4 (de Geus et al. 1990)
112	HD104901	0.5345	-6.1185	0.0832	0.93	34		7.3	oc	
113	HD106983	9.2402	-37.4306	-6.5761	2.27	482		6.8	oc	Sco-Cen assoc. (Gutierrez-Moreno & Moreno 1968)
114	HD108610	2.0141	-11.7086	-1.7007	0.97	22		7.4		Loden624 (Loden 1979)
115	HD110956	9.7326	-33.6266	-15.1050	1.65	689		6.9	oc	lower Centaurus Crux assoc. (Madsen et al. 2002)
116	HD112092	8.0152	-31.6310	-13.3530	1.93	450	y	6.9	oc	Sco OB2-4 (de Geus et al. 1990)
117	HD112244	0.7576	-5.9492	-1.0772	1.11	16		8.0		
118	HD113703	8.1592	-29.5581	-15.6923	0.97	530	y	6.9	oc	lower Centaurus Crux assoc. (de Geus et al. 1989)
119	HD113791	6.7962	-27.1183	-12.8082	1.06	18	y	7.0	oc	lower Centaurus Crux assoc. (de Geus et al. 1989)
120	HD114911	8.6760	-41.3442	-6.9604	3.32	164		6.8	oc	lower Centaurus Crux assoc. (de Geus et al. 1989)
121	HD117460	0.5184	-4.8616	-1.8820	0.81	30		7.2	oc	
122	HD119423	2.0923	-10.4423	-6.0397	0.81	27	y	7.5	oc	HIP67330 cluster (Platais et al. 1998)
123	HD120324	7.3269	-23.0395	-18.3608	5.78	432	y	6.9	oc	upper Centaurus-Lupus assoc. (de Geus et al. 1989))
124	HD120642	10.7449	-38.9967	-26.8626	1.10	70	y	7.0	oc	

Table 1. (Continued.)

125	HD120955	4.8225	-10.4278	-10.7098	1.28	12		8.1		upper Centaurus-Lupus assoc. (de Geus et al. 1989)
126	HD120991	1.4567	-7.6994	-4.2246	1.56	9		7.5		Sco OB2-3 (de Geus et al. 1990)
127	HD123445	6.2446	-20.3339	-17.6995	3.15	214		6.9	oc	upper Centaurus-Lupus assoc. (Madsen et al. 2002)
128	HD123635	1.7216	-9.8201	-5.2374	0.96	11	y	8.4		upper Centaurus-Lupus assoc. (Madsen et al. 2002)
129	HD124367	7.6043	-24.0073	-20.7365	1.10	145		7.0	oc	upper Centaurus-Lupus assoc. (de Geus et al. 1989)
130	HD124471	2.1003	-7.7062	-6.3589	1.20	34		8.0		Alessi 6 (Alessi et al. 2003)
131	HD126981	7.4763	-38.1376	-27.4689	0.92	33	y	7.5		upper Centaurus-Lupus assoc. (Madsen et al. 2002)
132	HD127971	9.2311	-21.7163	-21.3523	3.17	69		7.0		Sco OB2-3 (de Geus et al. 1990)
133	HD128819	6.5884	-19.7219	-21.8686	1.12	401	y	6.9	oc	upper Centaurus-Lupus assoc. (de Geus et al. 1989)
134	HD128919	0.9166	-2.9962	-3.5024	0.95	26	y	8.5		Alessi 6 (Alessi et al. 2003)
135	HD129791	8.2374	-19.1905	-30.2195	2.52	90	y	7.0		upper Centaurus-Lupus assoc. (de Geus et al. 1989)
136	HD131168	2.5091	-3.0294	-2.8016	1.10	16		7.6		
137	HD135160	1.2190	-2.9080	-2.9980	1.49	92		7.4	oc	Sco-Cen assoc. (Gutierrez-Moreno & Moreno 1968)
138	HD135240	1.4345	-4.0855	-3.7582	0.95	117		7.9	oc	
139	HD135591	1.2091	-3.1092	-3.7802	0.83	197	y	7.0	oc	
140	HD136454	1.8158	-9.5259	-7.6374	1.07	16	y	7.7		
141	HD138800	4.5583	-15.5173	-26.4079	1.50	19		7.8		
142	HD139619	2.0557	-3.4270	-3.2530	0.98	39		7.8	oc	
143	HD140022	1.4055	-2.5916	-4.6828	1.09	11		7.9		
144	HD141318	1.6512	-3.4460	-4.0672	0.76	74		7.8	oc	
145	HD141468	1.5433	-3.0336	-9.5324	0.91	8		8.6		
146	HD141569	8.9597	-17.4203	-19.1134	1.02	36	y	7.3		HD141569 group (Aarnio et al. 2008)
147	HD142448	5.9798	2.5541	-18.4483	2.95	20		7.8		
148	HD142514	4.3592	-10.8685	-5.5812	1.74	17		7.6		
149	HD143018	9.6733	-12.3994	-26.2102	2.44	49		7.2		upper Sco (Madsen et al. 2002)
150	HD143118	7.5942	-17.5932	-27.2556	2.98	522	y	6.9	oc	upper Centaurus-Lupus assoc. (de Geus et al. 1989)
151	HD143939	7.0329	-16.4972	-26.3131	1.02	446	y	6.9	oc	upper Centaurus-Lupus assoc. (Madsen et al. 2002)
152	HD145483	9.9483	-20.9182	-47.4156	2.41	33		7.9		upper Sco assoc. (de Geus et al. 1989)

Table 1. (Continued.)

153	HD148066	1.3412	-2.6437	-3.6085	0.96	18		8.1		
154	HD149249	1.0312	-2.0317	-2.4875	0.83	59		7.8	oc	
155	HD150742	5.7534	-12.0612	-21.6660	0.76	779		6.9	oc	upper Centaurus-Lupus assoc. (Madsen et al. 2002)
156	HD151158	0.4579	0.1300	-1.7868	4.16	8		6.8	oc	
157	HD152408	0.5417	-0.4744	-1.6173	0.83	28		6.3	oc	Sco OB1 (van Genderen et al. 1984)
158	HD152723	0.6772	0.2604	-0.1044	7.48	13		7.1	oc	Trumpler 24 (Heske & Wendker 1985)
159	HD152901	1.1231	0.3173	-2.8225	8.01	38		7.8	oc	
160	HD153519	1.0918	1.2137	0.1063	0.80	22		7.7		
161	HD153613	7.6564	-9.3364	-50.2467	1.25	76		7.6	oc	Sco OB2-1 (de Geus et al. 1990)
162	HD155240	1.6425	-3.0062	-7.4575	0.76	34		7.9		
163	HD156247	4.2326	-1.5463	-13.0234	2.00	22	y	7.5		
164	HD156325	2.6245	-1.6384	-7.2677	0.80	104		7.4	oc	Sco OB2-1 (de Geus et al. 1990)
165	HD157042	3.5613	-6.2087	-17.6990	0.99	36		7.6	oc	Sco OB2-1 (de Geus et al. 1990)
166	HD157246	3.9387	-3.5828	-12.6407	2.49	19		7.8		Sco OB2-1 (de Geus et al. 1990)
167	HD157736	6.1087	-5.9675	-41.6264	0.71	25	y	7.6		Sco OB2-1 (de Geus et al. 1990)
168	HD157741	5.8215	7.8400	10.6838	0.96	26	y	7.7		
169	HD159091	2.4701	-4.3272	-9.0284	1.30	53	y	7.6		Sco OB2-1 (de Geus et al. 1990)
170	HD159176	1.1666	2.6212	-0.7976	0.94	31		7.2	oc	
171	HD160281	1.1203	-0.7137	-1.5572	1.04	56	y	7.4	oc	
172	HD160957	2.1597	1.0658	-2.6290	1.71	71		8.1	oc	
173	HD160974	0.6428	-4.1802	-1.7463	0.75	9		6.8		
174	HD161004	1.9858	0.4035	-8.1727	0.82	38		7.4		
175	HD162082	2.8321	-0.4980	-7.2502	1.07	35	y	7.3		
176	HD163181	0.6959	2.6450	-1.7048	0.58	10		7.5		Sco OB2-1 (de Geus et al. 1990)
177	HD164492	0.6843	0.4208	-1.8631	0.74	28		6.9	oc	NGC 6514 (Ogura & Ishida 1975)
178	HD165493	3.5340	-4.1117	-17.9939	1.32	46	y	7.6		Alessi 9 (Alessi et al. 2003)
179	HD165530	3.5149	14.6275	-11.0215	1.14	8		8.6		
180	HD166182	2.8036	-2.0733	-6.5130	1.82	64		7.2	oc	
181	HD166563	6.0354	3.0563	-2.1337	0.95	35		7.6		
182	HD166566	0.5557	-0.3748	-2.8015	1.71	20		6.8	oc	Sgr OB6 (Mel’nik & Dambis 2017)

Table 1. (Continued.)

183	HD167771	0.6411	1.0938	-1.6952	0.79	50		7.1	oc	Sgr OB4 (Melnik & Dambis 2020)
184	HD170385	1.5331	1.1059	-3.5658	1.16	13		7.7		
185	HD170580	2.1477	-1.9520	-7.8909	1.36	26		7.7		
186	HD170740	4.4159	1.5470	-17.1479	1.00	33	y	7.5	oc	Sct OB2 (de Geus et al. 1990)
187	HD171247	2.9899	-0.2927	-9.6526	0.96	30		7.6		
188	HD173360	5.9620	0.2034	-28.2951	2.26	33		7.6		
189	HD174152	2.1672	2.5122	-2.8230	1.22	20	y	7.6		Sco OB2-1 (de Geus et al. 1990)
190	HD174585	2.6879	1.5397	-3.7209	1.12	226		7.3	oc	HIP 98321 cluster (Platais et al. 1998)
191	HD174638	3.5982	2.0451	-3.6847	3.24	134	y	7.2	oc	beta Lyr cluster (Bastian 2019)
192	HD176873	2.1563	0.5748	-10.2173	2.23	21	y	7.5		
193	HD177817	3.5139	-1.7503	-16.7440	1.22	15		7.7		
194	HD177880	2.3962	1.8385	-11.5577	0.96	18	y	7.4	oc	
195	HD179316	1.0749	-3.0403	-5.3960	1.39	31		8.2	oc	
196	HD179761	4.7730	10.1017	-0.8249	0.91	25		7.7		
197	HD180555	8.2599	0.0506	6.4602	3.43	19		7.8		
198	HD181454	8.3782	2.8902	-18.1253	3.11	16		7.7		
199	HD181558	4.4426	3.2216	-12.4379	1.08	71		7.7	oc	
200	HD182110	7.4854	5.4475	-31.7470	1.29	41	y	7.4		Ruprecht 147 (Cantat-Gaudin et al. 2018)
201	HD185507	4.1557	4.5279	-4.5067	0.77	29		7.6		
102	HD185514	2.4067	0.7139	-4.5722	2.02	23	y	7.7		Ruprecht 147 (Cantat-Gaudin et al. 2018)
203	HD194262	2.0214	1.9943	-6.6713	1.03	10	y	7.5		
204	HD195556	2.5459	10.0579	6.8728	0.84	13		7.6		
205	HD199218	3.0640	7.8349	0.7463	0.97	72	y	7.5	oc	
206	HD201819	1.0087	0.0141	0.3231	1.04	14	y	8.9		Cyg OB4 (Mel'nik & Dambis 2017)
207	HD222661	20.8948	98.5776	-66.2311	0.70	10	y	7.7		Pleiades supercluster (Eggen 1992)
208	HD224098	3.2668	-3.9287	-6.1142	0.85	13		7.9		

Following system does not belong to a cluster but the secondary is identified as common proper motion object to the primary. HD8803, HD60575, HD71304, HD71833, HD86388, HD112413, HD138497, HD212581.
binarity; y: secondary star in Gahm, Ahlin, and Lindroos (1983) is identified as the group member candidates.
cl; oc: cluster, none; association

Table 2. The candidates of the group members.

HD 560									
Gaia DR3	RA	Dec	Plx	PMra	PMdec	RUWE	G mag	B_{P} - R_P	A(G)
	[deg]	[deg]	[mas]	[mas yr^{-1}]	[mas yr^{-1}]	mag	mag	mag	
2780259775266087168	6.1608	14.8773	10.5002	26.7898	-2.3792	0.941	17.556	3.753	0.000
2774128103860691968	0.5359	18.9228	10.2500	35.6134	-2.2147	1.118	12.083	1.465	0.204
2772442655614620928	0.1765	16.3153	10.2487	32.5047	4.7034	1.033	17.956	3.543	0.000
2772754852491626368	1.8241	17.0066	10.1652	23.8171	7.2263	1.348	16.862	2.881	0.000
2557782805795380608	10.3828	8.0676	10.4387	34.7674	1.0527	8.369	11.228	1.217	0.000
2751675908917728640	8.7812	11.7209	11.9507	38.6837	4.3499	1.038	16.387	3.008	0.000
2747935542158907648	8.0992	6.9555	10.1557	26.4150	1.5926	4.065	5.680	0.001	0.144
2747935576518646144	8.1068	6.9564	11.4488	29.6829	5.9872	3.706	9.327	1.009	0.221
2753834044084699136	2.5101	11.1439	10.8148	31.5620	4.8117	0.809	10.096	1.001	0.001
2753834422041820928	2.5093	11.1458	11.0592	31.4929	2.6513	0.730	5.538	-0.088	0.001
2754437229291762944	6.0566	11.5082	10.7400	30.6102	3.0190	1.181	14.906	3.020	0.000
2756036881271133440	5.1323	13.4925	10.5025	24.1733	1.5582	1.156	13.295	1.959	0.000